

# Extensive weight loss can reduce immune age by altering IgG N-glycosylation

Valentina L Greto<sup>1\*</sup>, Ana Cvetko<sup>2\*</sup>, Tamara Štambuk<sup>3\*</sup>, Niall J Dempster<sup>4</sup>, Domagoj Kifer<sup>2</sup>, Helena Deriš<sup>3</sup>, Ana Cindrić<sup>3</sup>, Frano Vučković<sup>3</sup>, Mario Falchi<sup>5</sup>, Richard S Gillies<sup>6</sup>, Jeremy W Tomlinson<sup>4</sup>, Olga Gornik<sup>2,3</sup>, Bruno Sgromo<sup>6</sup>, Tim D Spector<sup>5</sup>, Cristina Menni<sup>5\*</sup>, Alessandra Geremia<sup>1\*</sup>, Carolina V Arancibia-Cárcamo<sup>1\*</sup>, Gordan Lauc<sup>2,3\*</sup>

<sup>1</sup>Translational Gastroenterology Unit and NIHR Oxford Biomedical Research Centre, Nuffield Department of Medicine, University of Oxford, United Kingdom

<sup>2</sup>Faculty of Pharmacy and Biochemistry, University of Zagreb, Zagreb, Croatia

<sup>3</sup>Genos Glycoscience Research Laboratory, Zagreb, Croatia

<sup>4</sup>Oxford Centre for Diabetes and NIHR Oxford Biomedical Research Centre, Endocrinology and Metabolism, Radcliffe Department of Medicine, University of Oxford, United Kingdom

<sup>5</sup>The Department of Twin Research, King's College London, St Thomas' Hospital, London, United Kingdom

<sup>6</sup>Department of Upper GI Surgery, Oxford University Hospitals, United Kingdom

\*The authors equally contributed to this work

Corresponding author:

Gordan Lauc

[glauc@pharma.hr](mailto:glauc@pharma.hr)

Faculty of Pharmacy and Biochemistry, University of Zagreb

A. Kovačića 1, 10 000 Zagreb, Croatia

1 **ABSTRACT**

2 **Background**

3 Obesity represents a global health threat, and is associated not only with exponentially  
4 increased cardiometabolic morbidity and mortality, but with adverse clinical outcomes in  
5 patients infected with SARS-CoV-2 as well. Enzymatic attachment of complex oligosaccharides  
6 to proteins (glycosylation) is highly responsive to numerous (patho)physiological conditions  
7 and ageing, which is perhaps best exemplified on IgG. The prospect of immune age reduction,  
8 by reverting induced glycosylation changes through metabolic intervention, opens many  
9 possibilities. Herein, we have investigated whether weight loss interventions affect  
10 inflammation- and ageing-related glycosylation alterations, in a longitudinal cohort of  
11 bariatric-surgery patients. To support potential findings, BMI-related glycosylation changes  
12 were monitored in a longitudinal TwinsUK cohort.

13 **Methods**

14 IgG and plasma N-glycans were chromatographically profiled in 37 obese patients, subjected  
15 to low-calorie diet and then to bariatric surgery, across multiple timepoints. Similarly, plasma  
16 glycome was analysed in 1,680 TwinsUK participants and longitudinally monitored during a  
17 20-year follow-up.

18 **Findings**

19 Low-calorie diet induced marked increase in low branched and significant decrease in highly  
20 branched, more complex plasma N-glycans – the change opposite to the one typically  
21 observed in inflammatory conditions. Bariatric surgery resulted in extensive, gradual  
22 alterations in IgG glycome, that accompanied progressive weight loss during one year follow-  
23 up. We observed significant increase in digalactosylated and sialylated, and substantial  
24 decrease in agalactosylated and core fucosylated IgG glycans. In general, such IgG glycan  
25 profile is associated with a younger biological age and reflects enhanced anti-inflammatory  
26 IgG potential. The TwinsUK cohort replicated weight loss-associated agalactosylation decrease  
27 and digalactosylation increase, estimated through BMI decrease over a 20-year-period.

28 **Interpretation**

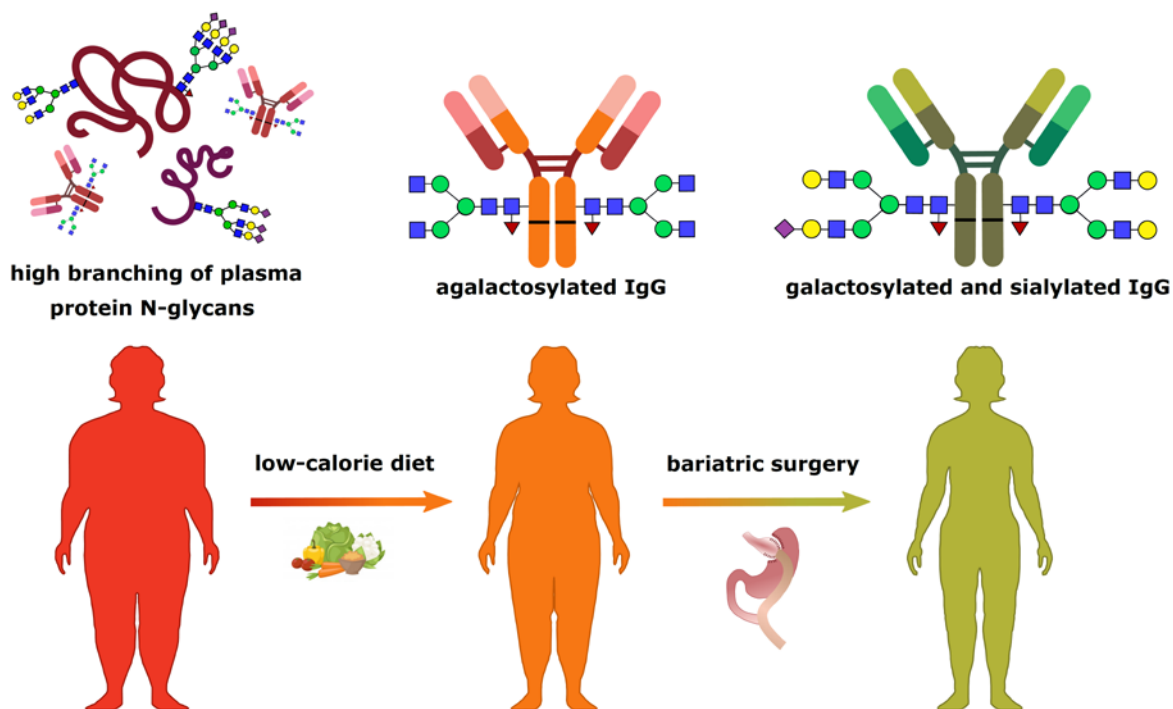
29 Altogether, these findings highlight that weight loss substantially affects both plasma and IgG  
30 N-glycosylation, resulting in improved biological and immune age.

31

32

33 **GRAPHICAL ABSTRACT**

34



35

36

37

38 **HIGHLIGHTS**

39

- 40 • Obesity is associated to circulating pro-inflammatory high branched N-glycans and  
41 IgG agalactosylation
- 42
- 43 • High branching of N-glycans from total plasma proteins decreases after 3-week low-  
44 calorie diet
- 45
- 46 • IgG galactosylation and sialylation increase after bariatric surgery-induced weight  
47 loss
- 48
- 49 • Decrease of BMI over time is associated to increased IgG galactosylation and a  
50 reduction of biological age

51

52

53 **KEYWORDS**

54 N-glycosylation; bariatric surgery; weight loss; immunoglobulin G; COVID-19; biological age

## 55 INTRODUCTION

56 The global prevalence of obesity has risen dramatically, to the point that it is now considered  
57 a pandemic (1). In the current collision with the emergent coronavirus disease (COVID-19  
58 pandemic), there is a strong association of obesity and older age with COVID-19 complications  
59 and severity (2). Moreover, US Centre for Disease Control and Prevention recently reported  
60 that obesity represents the highest risk factor for COVID-19 mortality in people younger than  
61 65 years (3). According to the World Health Organization, over 650 million individuals are  
62 obese, accounting for 13% of the world's adult population. Obesity confers a risk for metabolic  
63 syndrome, contributing to type 2 diabetes and cardiovascular disease (CVD) development (4).  
64 Metabolic syndrome is linked to a chronic systemic low-grade inflammation, which  
65 contributes to the aging of the immune system denoted as inflammaging (5,6). Obesity-  
66 related inflammaging results in impaired innate and adaptive immune function, and is  
67 characterized by high serum levels of IL-6, TNF- $\alpha$  and CRP (7). Moreover, this persistent  
68 inflammatory state may potentially lead to increased viral shedding and to delayed, blunted  
69 antiviral responses to SARS-CoV-2 infection (8,9).

70 Changes in protein N-glycosylation are one of the hallmarks of inflammaging (6,9). The human  
71 circulating N-glycome represents the entire set of glycans that are covalently attached to  
72 plasma proteins through a nitrogen on an asparagine residue. N-glycans are essential for life  
73 and are involved in many physiological processes (10), including signal transduction, protein  
74 trafficking and folding, receptor regulation and cell adhesion. Glycosylation has a fundamental  
75 role in the innate and adaptive immune responses, accentuated by the fact that all five classes  
76 of immunoglobulins (Ig) bear N-glycans. In this regard, IgG is probably the most investigated  
77 glycoprotein, whose effector functions are controlled by its Fc-bound glycans (11).

78 Inter-individual differences in the pace of biological ageing is an intriguing concept that tries  
79 to explain why some people stay healthy until very late chronological age, while others age  
80 faster and have shorter life expectancy. The same may apply for the risk of severe COVID-19.  
81 Progressive age-related changes of IgG glycosylation have been extensively studied (10,12,13),  
82 and the GlycanAge model has been proposed to express the difference between chronological  
83 ageing and IgG glycome ageing (14). The "age" of the IgG glycome might be estimated through  
84 the levels of agalactosylated species, which are increasing with ageing and are associated with  
85 enhanced immune activation (15). The opposite applies for digalactosylated IgG glycoforms,  
86 which are usually related to a younger age. Besides age-related changes, specific IgG

87 glycosylation patterns have been already associated with CVD risk score and subclinical  
88 atherosclerosis in two large independent UK cohorts (16). Moreover, a prospective follow-up  
89 of the EPIC-Potsdam cohort confirmed that changes in plasma N-glycome composition are  
90 predictive of future CVD events, with comparable predictive power to the American Heart  
91 Association (AHA) score in men and even better predictive power in women (17). The link  
92 between an “old”, proinflammatory IgG N-glycome and hypertension has also been  
93 profoundly studied (18–20), and similar IgG glycosylation patterns were associated with  
94 increased body mass index (BMI) and measures of central adiposity (21,22).

95 Studies on mouse models further corroborate the importance of differential IgG glycoforms  
96 in CVD pathogenesis. Namely, it has been shown that hyposialylated IgG (corresponding to an  
97 “old” IgG glycome) can induce obesity-related hypertension and insulin resistance in B-cell-  
98 deficient mice, through activation of the endothelial FcγRIIB (23,24). These findings indicate  
99 that the IgG N-glycome could represent more than a biomarker of inflammation and aging,  
100 since distinctive IgG glycoforms act as effector molecules in certain pathologies. Furthermore,  
101 supplementation with *N*-acetylmannosamine (ManNAc), a precursor of sialic acid, protects  
102 obese mice from hypertension and insulin resistance induction by reverting an “old” IgG N-  
103 glycome into a “young” one (24,25). However, studies exploring the possibilities of converting  
104 an “old” IgG glycome into a “young” one by metabolic intervention in humans are limited. Of  
105 note, only one small study indicated that high-intensity interval training can “rejuvenate” the  
106 IgG N-glycome (26).

107 Finally, severe obesity can be resolved only through bariatric surgery and subsequent weight  
108 loss (27). The resulting weight loss impacts energy balance and metabolism, contributing to  
109 the increased insulin response, improved glycaemic control and reduction of total body fat,  
110 leading to decreased CVD risk and mortality (28). In this study we aimed to determine whether  
111 weight loss affects glycan markers related to inflammation and ageing, in a longitudinally-  
112 monitored cohort of obese individuals undergoing low-calorie diet and then bariatric surgical  
113 interventions. In order to support potential findings, we also investigated the BMI-related  
114 glycosylation changes in a longitudinal TwinsUK cohort. The analysis of samples obtained from  
115 the largest longitudinal twins cohort in the UK allowed us to observe the changes of BMI in  
116 relation to the IgG N-glycosylation alterations over time.

117  
118

119 **METHODS**

120 **Study populations**

121 *Bariatric cohort.* The cohort included 37 participants, recruited at Oxford University Hospitals  
 122 to the Gastrointestinal Illnesses study (Ref: 16/YH/0247). All patients were characterised by  
 123 metabolic status and medical history. Bariatric patients were considered eligible in accordance  
 124 to National Institute for Health and Care Excellence (NICE) and local guidelines. The choice of  
 125 bariatric operation was decided according to the Oxford Bariatric Unit regular practice.  
 126 Patients with a history of alcoholism and/or ongoing anticoagulant treatment were excluded.  
 127 Patients were also excluded in case of pregnancy, active substance abuse or uncontrolled  
 128 psychiatric condition including eating disorders. Participants were sampled at baseline and  
 129 subjected to 3-week low calorie carbohydrate-restricted diet (900 cal, maximum 100 g of  
 130 carbohydrates per day), followed by bariatric surgery. The sequential follow-up timepoints  
 131 included the day of the surgery (baseline), after  $6.54 \pm 3.4$  months (mean  $\pm$  IQR) and  $12.47 \pm$   
 132  $6.55$  months post-op. Characteristics of the bariatric cohort are shown in Table 1.

133 **Table 1 Demographic characteristics of the bariatric cohort**

<i>Characteristics</i>	<i>Bariatric cohort</i>				
Total No. of participants (N)	37				
No. of participants Sleeve Gastrectomy (SG), N (%)	25 (68%)				
No. Roux-en-Y Gastric Bypass RYGB N (%)	12 (32%)				
No. of participants each timepoint (N)	Pre-op low-calorie diet	Time of surgery	1st post-op timepoint	2 <sup>nd</sup> post-op timepoint	
	8	37	30	24	
BMI* each timepoint, mean $\pm$ SD, kg/m <sup>2</sup>	Before diet	End of diet	Time of surgery	1 <sup>st</sup> post-op timepoint	2 <sup>nd</sup> post-op timepoint
	48.53 $\pm$ 4.13	46.60 $\pm$ 4.21	46.21 $\pm$ 4.75	36.01 $\pm$ 5.07	32.82 $\pm$ 5.17
Female, sex, N (%)	33 (89%)				
Type 2 diabetes, N (%)	6 (16%)				

134  
 135 \*BMI reference values: <18.5 (underweight), 18.5–24.9 (normal weight), 25–29.9  
 136 (overweight), >30 (obese).

137  
 138 *TwinsUK cohort.* We have analysed a total of 6,032 plasma samples from 2,146 participants of  
 139 the TwinsUK study, collected at multiple timepoints over a 20 year-period (29). These included  
 140 1,865 individuals sampled at 3 timepoints, 156 individuals sampled at 2 timepoints and 125  
 141 individuals sampled only once. Following the plasma N-glycome analysis, glycan data

142 underwent quality control (see *Statistical analysis* section), which decreased the dataset to  
143 5,889 samples (measurements). Out of these 5,889 measurements, we have proceeded with  
144 statistical analysis on a subset of 3,742 samples (measurements) which had information on  
145 BMI available. Description of the TwinsUK cohort is provided in Table 2.

146 **Table 2 Demographic characteristics of the TwinsUK cohort**

<i>Characteristics</i>	<i>TwinsUK cohort (BMI subset)</i>
No. of participants (N)	1,680
No. of glycan measurements (N)	3,742
Baseline age, mean $\pm$ SD, years	53.23 $\pm$ 10.86
Follow up time, mean $\pm$ SD, years	7.90 $\pm$ 5.66
Female sex, N (%)	1,680 (100)
Baseline BMI, mean $\pm$ SD, kg/m <sup>2</sup>	25.45 $\pm$ 4.53

147

#### 148 **Ethical statement**

149 Ethical approval for the study was obtained by the National Research Ethics Committees of  
150 the UK National Health Service (NHS) under the reference number 16/YH/0247. All individuals  
151 participating in this study gave written informed consent. The TwinsUK study was approved  
152 by NRES Committee London–Westminster, and all twins provided informed written consent.

#### 153 **N-glycome analysis**

##### 154 *Isolation of IgG from human plasma*

155 IgG was isolated from plasma samples by affinity chromatography as described previously  
156 (30). In brief, IgG was isolated in a high-throughput manner, using 96-well protein G  
157 monolithic plates (BIA Separations, Slovenia), starting from 100  $\mu$ l of plasma. Plasma was  
158 diluted 7 $\times$  with phosphate buffered saline (PBS; Merck, Germany) and applied to the protein  
159 G plate. IgG was eluted with 1 ml of 0.1 M formic acid (Merck, Germany) and immediately  
160 neutralized with 1 M ammonium bicarbonate (Acros Organics, USA).

##### 161 *N-glycan release from IgG and total plasma proteins*

162 Isolated IgG samples were dried in a vacuum centrifuge. After drying, IgG was denatured with  
163 the addition of 30  $\mu$ l of 1.33% SDS (w/v) (Invitrogen, USA) and by incubation at 65  $^{\circ}$ C for 10  
164 min. Plasma samples (10  $\mu$ l) were denatured with the addition of 20  $\mu$ l of 2% (w/v) SDS  
165 (Invitrogen, USA) and by incubation at 65  $^{\circ}$ C for 10 min. From this point on, the procedure was



166 identical for both IgG and plasma samples. After denaturation, 10 µl of 4% (v/v) Igepal-CA630  
167 (Sigma Aldrich, USA) was added to the samples, and the mixture was shaken 15 min on a plate  
168 shaker (GFL, Germany). N-glycans were released with the addition of 1.2 U of PNGase F  
169 (Promega, USA) and overnight incubation at 37 °C.

#### 170 Fluorescent labelling and HILIC SPE clean-up of released N glycans

171 The released N-glycans were labelled with 2-aminobenzamide (2-AB). The labelling mixture  
172 consisted of 2-AB (19.2 mg/ml; Sigma Aldrich, USA) and 2-picoline borane (44.8 mg/ml; Sigma  
173 Aldrich, USA) in dimethyl sulfoxide (Sigma Aldrich, USA) and glacial acetic acid (Merck,  
174 Germany) mixture (70:30 v/v). To each sample 25 µl of labelling mixture was added, followed  
175 by 2 h incubation at 65 °C. Free label and reducing agent were removed from the samples  
176 using hydrophilic interaction liquid chromatography solid-phase extraction (HILIC-SPE). After  
177 incubation samples were brought to 96% of acetonitrile (ACN) by adding 700 µl of ACN (J.T.  
178 Baker, USA) and applied to each well of a 0.2 µm GHP filter plate (Pall Corporation, USA).  
179 Solvent was removed by application of vacuum using a vacuum manifold (Millipore  
180 Corporation, USA). All wells were prewashed with 70% ethanol (Sigma-Aldrich, St. Louis, MO,  
181 USA) and water, followed by equilibration with 96% ACN. Loaded samples were subsequently  
182 washed 5× with 96% ACN. N-glycans were eluted with water and stored at – 20 °C until usage.

#### 183 Hydrophilic interaction liquid chromatography of N glycans

184 Fluorescently labelled N-glycans were separated by hydrophilic interaction liquid  
185 chromatography (HILIC) on Acquity UPLC H-Class instrument (Waters, USA) consisting of a  
186 quaternary solvent manager, sample manager and a fluorescence detector, set with excitation  
187 and emission wavelengths of 250 and 428 nm, respectively. The instrument was under the  
188 control of Empower 3 software, build 3471 (Waters, Milford, USA). Labelled N-glycans were  
189 separated on a Waters BEH Glycan chromatography column, with 100 mM ammonium  
190 formate, pH 4.4, as solvent A and ACN as solvent B. In the case of IgG N-glycans, separation  
191 method used linear gradient of 75–62% acetonitrile at flow rate of 0.4 ml/min in a 27-min  
192 analytical run. For plasma protein N-glycans separation method used linear gradient of 70–  
193 53% acetonitrile at flow rate of 0.561 ml/min in a 25-min analytical run. The system was  
194 calibrated using an external standard of hydrolysed and 2-AB labelled glucose oligomers from  
195 which the retention times for the individual glycans were converted to glucose units (GU).  
196 Data processing was performed using an automatic processing method with a traditional  
197 integration algorithm after which each chromatogram was manually corrected to maintain



198 the same intervals of integration for all the samples. The chromatograms were all separated  
199 in the same manner into 24 peaks (GP1– GP24) for IgG N-glycans and 39 peaks (GP1–GP39)  
200 for plasma protein N-glycans and are depicted in Supplementary Figure 1 and Supplementary  
201 Figure 2, respectively. Detailed description of glycan structures corresponding to each glycan  
202 peak is presented in Supplementary Table 1. Glycan peaks were analysed based on their  
203 elution positions and measured in glucose units, then compared to the reference values in the  
204 “GlycoStore” database (available at: <https://glycostore.org/>) for structure assignment. The  
205 amount of glycans in each peak was expressed as a percentage of the total integrated area.  
206 For IgG glycans, in addition to 24 directly measured glycan traits, 8 derived traits were  
207 calculated, while for plasma glycans, in addition to 39 directly measured glycan traits, 16  
208 derived traits were also calculated. These derived traits average particular glycosylation  
209 features, such as galactosylation, fucosylation, bisecting GlcNAc, and sialylation. Formulas for  
210 IgG and plasma protein N-glycan derived traits for bariatric cohort are presented in  
211 Supplementary Table 2 and Supplementary Table 3, respectively. Derived trait calculations for  
212 TwinsUK cohort are presented in Supplementary Table 4.

### 213 **Statistical analysis**

214 *Bariatric cohort.* In order to remove experimental variation from the measurements,  
215 normalization and batch correction were performed on the UPLC glycan data. To make  
216 measurements across samples comparable, normalization by total area was performed. Prior  
217 to batch correction, normalized glycan measurements were log-transformed due to right-  
218 skewness of their distributions and the multiplicative nature of batch effects. Batch correction  
219 was performed on log-transformed measurements using the ComBat method (R package *sva*  
220 (31), where the technical source of variation (which sample was analysed on which plate) was  
221 modelled as batch covariate. To correct measurements for experimental noise, estimated  
222 batch effects were subtracted from log-transformed measurements.

223 Longitudinal analysis of patient samples through their observation period was performed by  
224 implementing a linear mixed effects model, where time was modelled as fixed effect, while  
225 the individual ID was modelled as random effect. Prior to the analyses, glycan variables were  
226 all transformed to standard Normal distribution by inverse transformation of ranks to  
227 Normality (R package “GenABEL”, function *rntransform*). Using rank transformed variables  
228 makes estimated effects of different glycans comparable, as these will have the same  
229 standardized variance. False discovery rate (FDR) was controlled by the Benjamini-Hochberg

230 procedure at the specified level of 0.05. Data was analysed and visualized using R  
231 programming language (version 3.5.2)(32).

232 *TwinsUK cohort*. Normalization of peak intensities to the total chromatogram area was  
233 performed for each measured sample separately. Calculated proportions were then batch  
234 corrected using ComBat method (R package *sva*)(31). After the batch correction the first 11  
235 peaks, which predominantly originate from IgG (33), were used to calculate 6 derived glycan  
236 traits – agalactosylation (G0), monogalactosylation (G1), digalactosylation (G2), bisecting  
237 GlcNAc (B), core fucosylation (CF) and high mannose structures (HM). Mixed models were  
238 fitted to estimate the effect of BMI change on IgG N-glycome (R package *lme4*)(34). Directly  
239 measured or derived glycan trait was used as a dependent variable in the mixed model. To  
240 differentiate between BMI change and the absolute BMI value, the variable was separated to  
241  $BMI_{baseline}$  and  $BMI_{difference}$  (calculated according to the following equation:  $BMI_{difference} =$   
242  $BMI_{follow\ up\ age} - BMI_{baseline\ age}$ ), and both were used in the model as a fixed effect. Since  
243 IgG N-glycome is affected by aging, age was included both as a fixed effect and a random  
244 slope. Finally, to meet the independency criteria, family ID and individual ID (nested within  
245 family) were included in the model as a random intercept. Due to multiple model fitting (for  
246 11 directly measured and 6 derived glycan traits) false discovery rate was controlled using  
247 Benjamini-Hochberg method. All statistical analyses were performed using R programming  
248 language (version 3.6.3)(32).

249

## 250 RESULTS

### 251 **Pre-surgical low-calorie diet extensively changes plasma N-glycome**

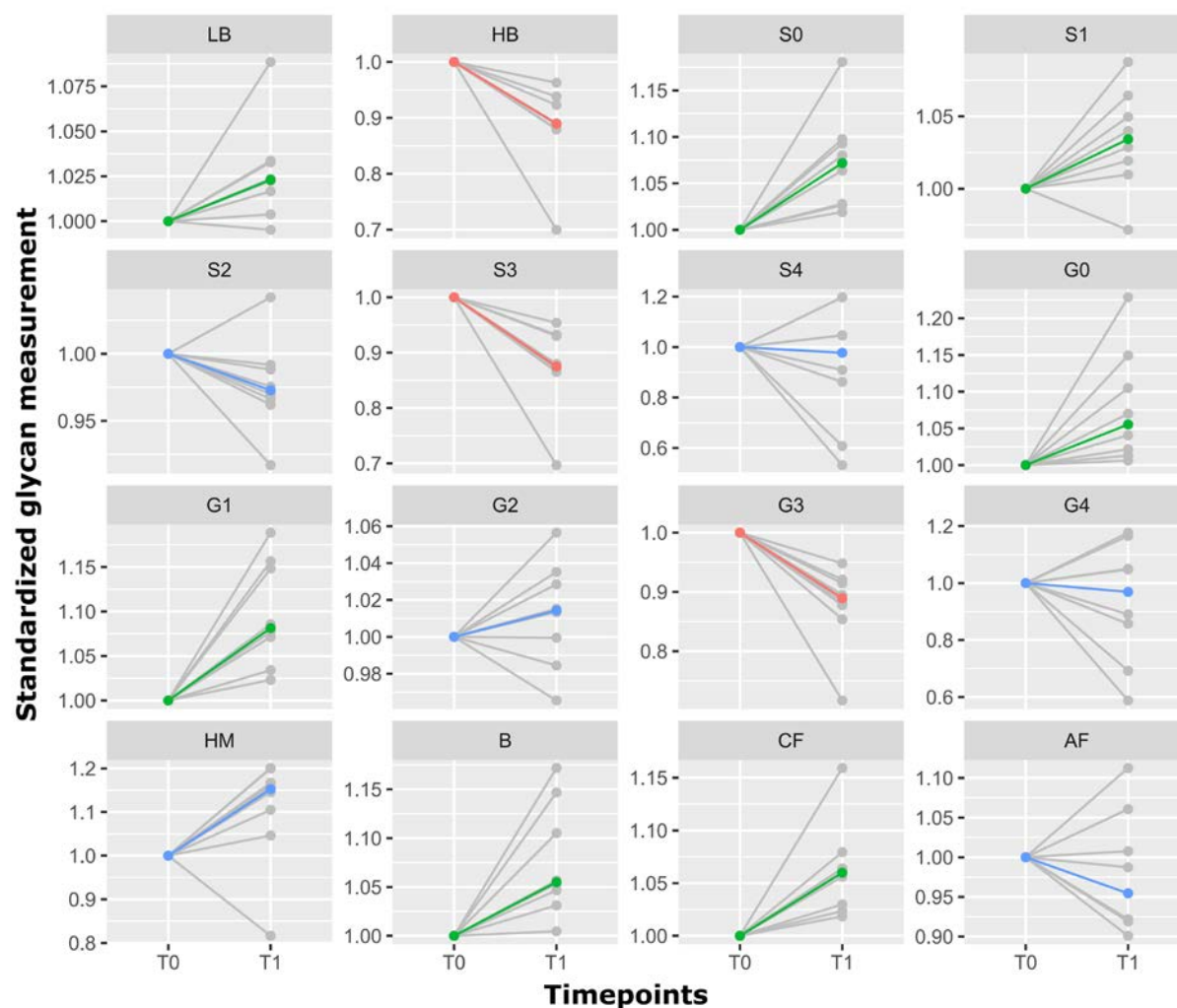
252 We profiled both plasma and IgG N-glycome in a cohort of bariatric surgery-candidate patients  
253 at the beginning and at the end of their pre-operative diet. We calculated corresponding  
254 derived glycan traits, which average particular glycosylation features. By employing a linear  
255 mixed model, we observed ample changes in plasma N-glycome, as 10 out of 16 calculated  
256 derived traits displayed significant alterations after the low-calorie diet. Namely, low  
257 branched (LB), agalactosylated (G0), monogalactosylated (G1), asialylated (S0),  
258 monosialylated (S1), core fucosylated (CF) and glycans bearing a bisecting GlcNAc (B) showed  
259 a substantial increase in their abundances (Table 3). Conversely, high branched (HB),  
260 trisialylated (S3) and trigalactosylated (G3) glycan abundances decreased (Table 3).  
261 Interestingly, IgG glycome was not affected by the low-calorie diet, as its derived traits did not

262 display any significant changes after the dieting period. Graphical representation of the  
 263 longitudinal alterations in plasma N-glycome after low calorie diet are depicted in Figure 1.

264 **Table 3 Low-calorie diet induces significant changes in plasma N-glycome.** Longitudinal  
 265 analysis was performed by implementing a linear mixed effects model, with time as a fixed  
 266 effect and the individual sample measurement as a random effect. False discovery rate was  
 267 controlled using Benjamini-Hochberg method at the specified level of 0.05.

<i>Derived glycan trait</i>	<i>Time_effect</i>	<i>Time_SE</i>	<i>Time_p-value</i>	<i>Adjusted p-value</i>
monogalactosylation (G1)	0.6020	0.0796	4.18 x10 <sup>-05</sup>	6.69 x10 <sup>-04</sup>
trisialylation (S3)	-1.1512	0.2008	3.04 x10 <sup>-04</sup>	2.43 x10 <sup>-03</sup>
agalactosylation (G0)	0.4903	0.0948	6.09 x10 <sup>-04</sup>	2.44 x10 <sup>-03</sup>
core fucosylation (CF)	0.5431	0.1011	4.73 x10 <sup>-04</sup>	2.44 x10 <sup>-03</sup>
high branching (HB)	-1.1925	0.2468	9.43 x10 <sup>-04</sup>	2.52 x10 <sup>-03</sup>
asialylation (S0)	0.6336	0.1310	9.40 x10 <sup>-04</sup>	2.52 x10 <sup>-03</sup>
trigalactosylation (G3)	-1.1925	0.2581	1.24 x10 <sup>-03</sup>	2.84 x10 <sup>-03</sup>
bisecting GlcNAc (B)	0.5457	0.1350	2.84 x10 <sup>-03</sup>	5.69 x10 <sup>-03</sup>
low branching (LB)	0.9839	0.3060	9.99 x10 <sup>-03</sup>	1.78 x10 <sup>-02</sup>
monosialylation (S1)	0.5024	0.1981	2.98 x10 <sup>-02</sup>	4.77 x10 <sup>-02</sup>
disialylation (S2)	-0.4314	0.1941	4.99 x10 <sup>-02</sup>	7.25 x10 <sup>-02</sup>
high mannose (HM)	0.7545	0.3619	6.24 x10 <sup>-02</sup>	8.33 x10 <sup>-02</sup>
antennary fucosylation (AF)	-0.1804	0.1102	1.28 x10 <sup>-01</sup>	1.58 x10 <sup>-01</sup>
digalactosylation (G2)	0.3107	0.2309	2.01 x10 <sup>-01</sup>	2.30 x10 <sup>-01</sup>
tetragalactosylation (G4)	-0.3446	0.3477	3.36 x10 <sup>-01</sup>	3.58 x10 <sup>-01</sup>
tetrasialylation (S4)	-0.3049	0.3547	4.00 x10 <sup>-01</sup>	4.00 x10 <sup>-01</sup>

268 Red – significant decrease; green – significant increase; blue – non-significant change.  
 269 GlcNAc – N-acetylglucosamine; SE – standard error



270

271 **Figure 1 Low calorie diet-related alterations in plasma N-glycome after a 3-week follow-up.**

272 Red line – significant decrease; green line – significant increase; blue line – non-significant

273 change.

274 **Bariatric surgery markedly alters IgG N-glycosylation**

275 Using the same chromatographic approach, we analysed samples from patients who

276 underwent bariatric surgery. The plasma samples were collected on the day of surgery (month

277 0), approximately 6 months post-surgery and 12 months post-surgery. Both plasma and IgG

278 N-glycans were profiled in each of these timepoints, and the obtained values were used for

279 derived glycan traits calculations. Of the examined plasma glycosylation features, only

280 agalactosylation (G0) displayed significant decrease after bariatric surgery (Table 4). On the

281 other hand, IgG N-glycome showed more extensive changes, following the bariatric

282 procedure. Namely, four out of eight tested derived traits showed marked changes: core

283 fucosylated (CF) and agalactosylated (G0) glycans decreased, while digalactosylated (G2) and

284 monosialylated (S1) glycans increased after the surgery (Table 4). The IgG glycans whose

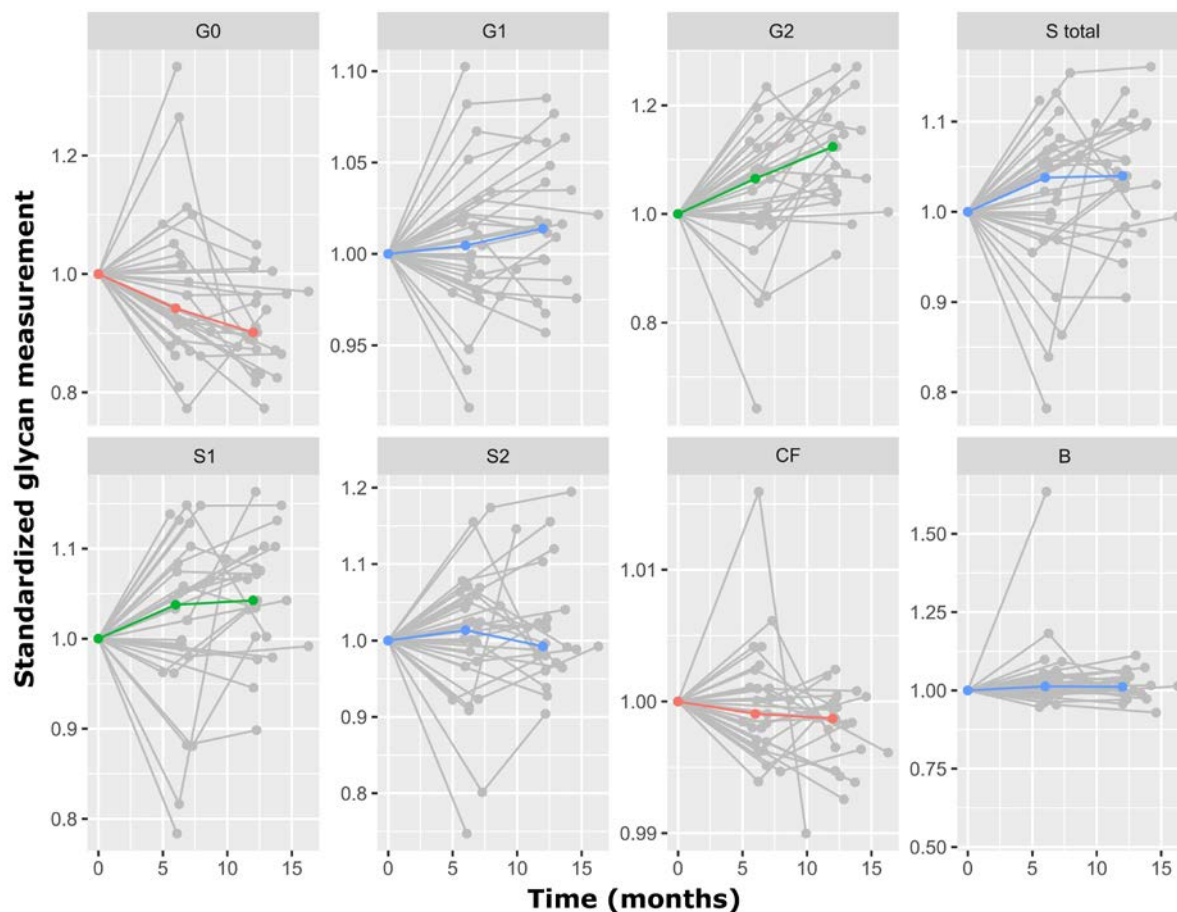
285 abundances were increased after bariatric surgery are major components of a “young” IgG  
 286 glycome, as they are typically associated with a younger age. The opposite applies to  
 287 agalactosylated structures, which are usual denominators of an “old” IgG glycome profile. We  
 288 also examined the correlation of patients’ clinical data with plasma and IgG glycome features  
 289 using multivariate analysis, but found no statistically significant associations (data not shown).  
 290 Finally, the type of bariatric surgery (either sleeve gastrectomy or Roux-en-Y gastric bypass)  
 291 did not affect plasma nor IgG glycome composition. Graphical representations of the  
 292 longitudinal alterations in IgG and plasma glycosylation features are depicted in Figure 2 and  
 293 Supplementary Figure 3, respectively.

294 **Table 4 Bariatric surgery induces significant changes in plasma and IgG N-glycomes.**

295 Longitudinal analysis was performed by implementing a linear mixed effects model, with  
 296 time as a fixed effect and the individual sample measurement as a random effect. False  
 297 discovery rate was controlled using Benjamini-Hochberg method at the specified level of  
 298 0.05.

<i>N-glycome</i>	<i>Derived glycan trait</i>	<i>Time_effect</i>	<i>Time_SE</i>	<i>Time_p-value</i>	<i>Adjusted p-value</i>
plasma	agalactosylation (G0)	-0.0273	0.0071	5.26x10 <sup>-04</sup>	8.42x10 <sup>-03</sup>
IgG	agalactosylation (G0)	-0.0339	0.0078	9.23x10 <sup>-05</sup>	7.38x10 <sup>-04</sup>
IgG	digalactosylation (G2)	0.0275	0.0072	3.75x10 <sup>-04</sup>	1.50x10 <sup>-03</sup>
IgG	monosialylation (S1)	0.0193	0.0080	1.97x10 <sup>-02</sup>	3.94x10 <sup>-02</sup>
IgG	core fucosylation (CF)	-0.0155	0.0064	1.74x10 <sup>-02</sup>	3.94x10 <sup>-02</sup>

299 Red – significant decrease; green – significant increase. SE – standard error.



300

301 **Figure 2 Bariatric surgery-related alterations in IgG N-glycome over time (months).** Red line  
302 – significant decrease; green line – significant increase; blue line – non-significant change.

303 **Weight loss induces shift towards “young” IgG N-glycome**

304 Using the same chromatographic approach, we profiled plasma protein N-glycome from 1,680  
305 TwinsUK study participants sampled at several timepoints over a 20-year-period. This served  
306 as a replication of the findings from the bariatric cohort, whose participants exhibited the  
307 reversal from “old” to “young” IgG N-glycome due to weight loss. As these results showed  
308 prominent changes in IgG composite glycan traits only, herein we focused on IgG glycosylation  
309 changes. Due to the fact that for TwinsUK cohort plasma glycome was profiled, we calculated  
310 derived traits and performed statistical analysis only on the first 11 glycan peaks,  
311 corresponding to the glycans predominantly originating from IgG (33). Six derived traits were  
312 calculated – agalactosylation (G0), monogalactosylation (G1), digalactosylation (G2),  
313 incidence of bisecting GlcNAc (B), core fucosylation (CF) and incidence of high mannose  
314 structures (HM). We examined IgG glycome alterations associated with changes in BMI using  
315 a mixed model on a subset of 3,742 samples. Out of six examined IgG glycosylation features  
316 (derived traits), three displayed significant BMI-related changes – agalactosylation (G0),



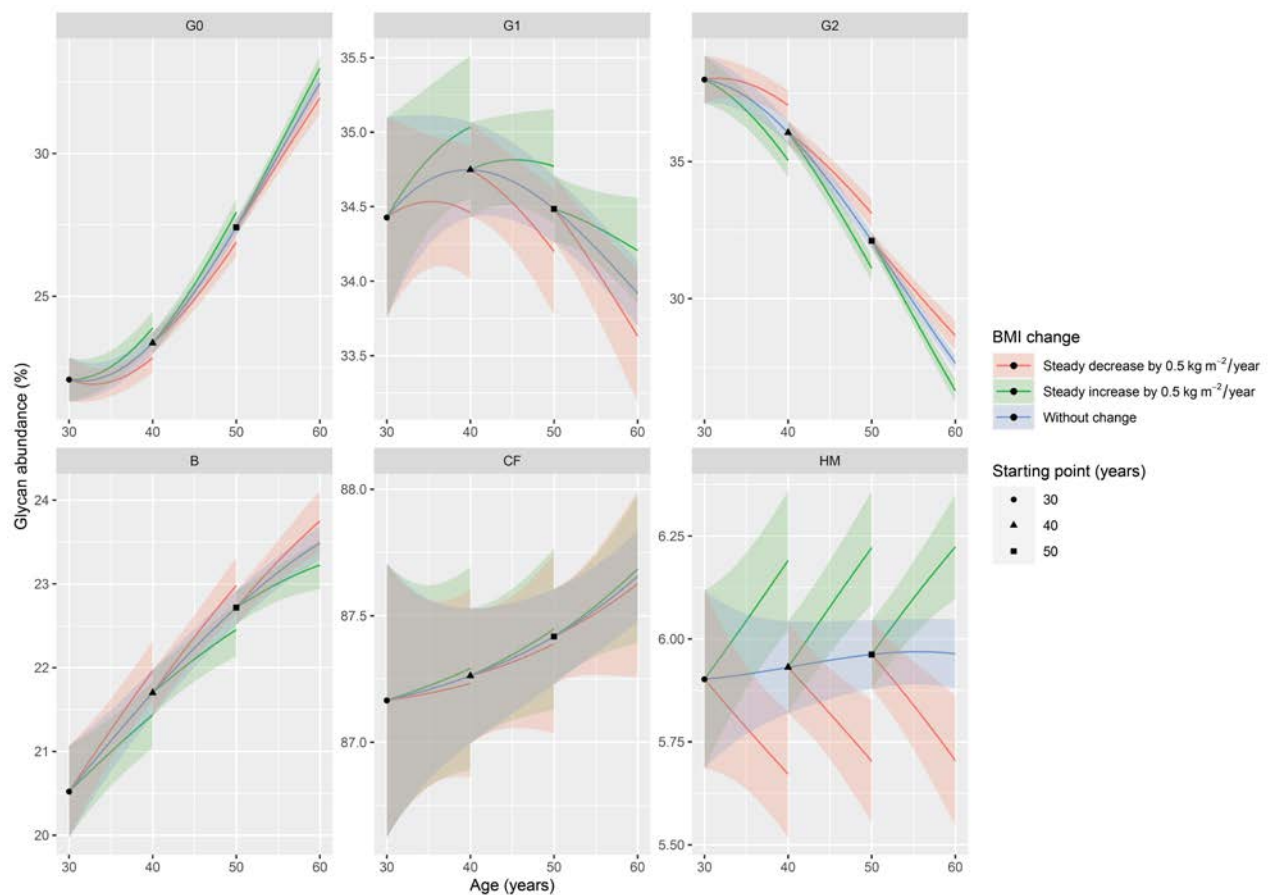
317 digalactosylation (G2) and incidence of high mannose structures (HM) (Table 5). Namely, the  
 318 abundance of digalactosylated (G2) glycans increased with the BMI decrease, while the  
 319 abundance of agalactosylated (G0) and high mannose glycans (HM) decreased with the weight  
 320 loss, estimated by the BMI drop. These findings are in line with the results observed in the  
 321 bariatric surgery cohort. Graphical representation of the longitudinal BMI-dependent  
 322 alterations of IgG glycosylation are depicted at Figure 3.

323 **Table 5 Longitudinally monitored weight loss results with significant changes of IgG N-**  
 324 **glycosylation.** Longitudinal analysis was performed by implementing a mixed model, fitted  
 325 to estimate the effect of BMI change on IgG N-glycome. False discovery rate was controlled  
 326 using Benjamini-Hochberg method at the specified level of 0.05.

<i>Derived glycan trait</i>	<i>BMI difference effect (glycan abundance (%) change per 1 kgm<sup>-2</sup> decrease in BMI)</i>	<i>BMI difference SE (glycan abundance (%) change per 1 kgm<sup>-2</sup> decrease in BMI)</i>	<i>p-value</i>	<i>Adjusted p-value</i>
digalactosylation (G2)	0.2004	0.0403	6.88x10 <sup>-07</sup>	5.85 x10 <sup>-06</sup>
high mannose (HM)	-0.0519	0.0119	1.33x10 <sup>-05</sup>	5.66 x10 <sup>-05</sup>
agalactosylation (G0)	-0.1048	0.0397	8.43x10 <sup>-03</sup>	1.79 x10 <sup>-02</sup>
bisecting GlcNAc (B)	0.0526	0.0262	4.49x10 <sup>-02</sup>	6.94x10 <sup>-02</sup>
monogalactosylation (G1)	-0.0573	0.0343	9.53x10 <sup>-02</sup>	1.25x10 <sup>-01</sup>
core fucosylation (CF)	-0.0059	0.0285	8.36x10 <sup>-01</sup>	8.89x10 <sup>-01</sup>

327 Red – significant decrease; green – significant increase; blue – non-significant change.  
 328 GlcNAc – N-acetylglucosamine; SE – standard error





329

330 **Figure 3 BMI-associated alterations in IgG N-glycosylation across multiple timepoints.**

331 Changes in IgG derived traits are presented with lineplots of hypothetical ageing of TwinsUK  
332 participants (all women). Black dot represents a starting point of a 30-year-old woman, black  
333 triangle of a 40-year-old woman and black square of a 50-year-old woman. All of these women  
334 have a baseline BMI of 25 kg m<sup>-2</sup>. Blue lines represent age-related IgG glycosylation changes  
335 attributed to stable BMI. Green lines represent age-related IgG glycosylation changes  
336 attributed to increasing BMI (0.5 kg m<sup>-2</sup> per year, through a period of 10 years). Red lines  
337 represent age-related IgG glycosylation changes attributed to decreasing BMI (0.5 kg m<sup>-2</sup> per  
338 year, through a period of 10 years). Highlighted areas represent 95% confidence intervals. The  
339 effect of age on IgG glycosylation is represented with the curve slope, while the effect of BMI  
340 change is represented with the distance of green/red line from the blue line.

341

## 342 **DISCUSSION**

343 In this study, we have observed extensive changes in both plasma and IgG N-glycome  
344 associated with weight loss following low-calorie diet and bariatric surgery, or expressed  
345 through BMI decrease. To the best of our knowledge, this is the first study to investigate

346 plasma and IgG N-glycome alterations in patients who underwent a low-calorie diet followed  
347 by bariatric surgery.

348 Prior to bariatric surgery, patients were subjected to a low-calorie diet which caused  
349 significant and extensive changes to the plasma protein N-glycome. The observed changes can  
350 be summarized as significant increase in low-branched, biantennary structures (S0, S1, G0,  
351 G1...) and, conversely, substantial decrease in high-branched, triantennary, more complex  
352 structures (S3, G3). The glycosylation alterations induced by a low-calorie diet are showing  
353 exactly the opposite direction of change than those seen in various inflammatory conditions,  
354 such as type 2 diabetes, chronic obstructive pulmonary disease and inflammatory bowel  
355 disease (17,30,35,36), suggesting a gradual attenuation of inflammation. Interestingly, no  
356 significant changes were found for the IgG N-glycome alone after the diet, probably due to  
357 the relatively short follow-up period (3 weeks), which matches IgG serum half-life. Altogether,  
358 our glycomic data suggest that the overall inflammatory body status improves after a short  
359 time of low-calorie diet, reflecting a quickly noticeable and beneficial metabolic effect.

360  
361 We have analysed both plasma and IgG N-glycome from individuals who underwent bariatric  
362 surgery, in a longitudinal manner. We observed significant changes in both plasma and IgG N-  
363 glycome. In particular, plasma N-glycome showed significant alterations only in  
364 agalactosylated (G0) glycans, whose abundance decreased during the follow-up period. Since  
365 the majority of agalactosylated species in plasma originates from IgG (33), it is no surprise that  
366 this glycosylation feature was also found to be significantly decreased in IgG glycome analysis.  
367 Elevated levels of G0 IgG glycoforms are typically associated with aging, pro-inflammatory IgG  
368 glycan profile and various inflammatory diseases (12). On the other hand, the levels of  
369 digalactosylated (G2) glycans increased after bariatric surgery and at sequential timepoints, in  
370 accordance with a reduced inflammatory potential of the circulating IgG. Interestingly, the  
371 increased levels of IgG galactosylation are associated with a younger biological age and are  
372 considered, in a way, as a measure of an individual's well-being (15). Conversely, IgG  
373 galactosylation levels substantially decrease with ageing and during inflammation (12,14). Our  
374 results demonstrate that weight loss, resulting from bariatric surgery, can initiate the reversal  
375 from an "old" to a "young" IgG N-glycome, potentially reversing the clock for the  
376 immune/biological age. Furthermore, bariatric surgery also resulted in significant IgG glycome  
377 alteration inducing a decrease in core fucosylation. The vast majority of circulating IgG

378 molecules bears core fucose (approximately 95%), which profoundly decreases IgG binding  
379 affinity to Fc $\gamma$ RIIIA receptor and sequential antibody-dependent cellular cytotoxicity (ADCC)  
380 (37). ADCC is largely mediated by natural killer cells that can lyse target cells and fight viral  
381 infections. This would suggest that an extensive weight loss ameliorates immune responses  
382 dedicated to combat viral infections, by altering IgG glycosylation and modulating its effector  
383 functions. Lastly, bariatric surgery-related weight loss led to an increase in IgG sialylation,  
384 which is the main modulator of the IgG anti-inflammatory actions (38). In addition to its anti-  
385 inflammatory actions, the level of IgG sialylation has been implicated in the pathogenesis of  
386 obesity-induced insulin resistance and hypertension, as already mentioned (23,24). Namely,  
387 inhibitory IgG receptor Fc $\gamma$ RIIB was found to be expressed in the microvascular endothelium.  
388 Sequentially, it was shown that hyposialylated IgG acts as its operating ligand, leading to the  
389 induction of obesity-related insulin resistance and hypertension. On the other hand, the  
390 sialylated glycoform is not activating the signalling pathways responsible for the insulin  
391 resistance and hypertension development, but is rather preserving insulin sensitivity and  
392 normal vasomotor tone, even in obese mice. Interestingly, the same group made another  
393 significant discovery – promotion of IgG sialylation breaks the link between obesity and  
394 hypertension/insulin resistance (24,25). Namely, supplementation with the sialic acid  
395 precursor restored IgG sialylation, highlighting a potential approach to improve both  
396 metabolic and cardiovascular health in humans, with a single intervention. Our data suggest  
397 that a similar effect might be achieved by weight loss interventions, through restoring of IgG  
398 sialylation levels. Altogether, it is remarkable that such profound effects were observed on a  
399 rather small number of participants, which further highlights their significance in a given  
400 biological setting.

401  
402 Lastly, in order to confirm the effects of weight loss on the biological/immune age, we  
403 investigated how BMI decrease affects IgG N-glycome during a 20-year-period. We observed  
404 the prominent inverse changes of agalactosylated (G0) and digalactosylated (G2) IgG glycans.  
405 Namely, agalactosylated IgG glycans significantly decreased, while digalactosylated ones  
406 substantially increased as the BMI decreased. These observations corroborated our earlier  
407 findings, confirming that the body weight reduction reverses IgG glycome from “old” to  
408 “young”, implying at the same time a likely reduction in the biological/ immune age.  
409 Nonetheless, we have to acknowledge the following limitations of TwinsUK as a replication

410 cohort: first – TwinsUK participants have not experienced such an extensive weight loss, which  
411 potentially influenced the replication of other significant glycan changes from the bariatric  
412 cohort; second – herein, the weight loss was approximated by BMI decrease, which is usually  
413 a legitimate assumption, however, it does not have to apply to all cases; and third – herein we  
414 profiled plasma glycome, while the IgG glycan traits were only approximated and the  
415 information on IgG sialylation was confounded by other plasma glycoproteins. Ideally, these  
416 issues could be circumvented in the future studies whose experimental design would allow  
417 the simultaneous, multi-centre follow-up of larger groups of patients.

418 Intense physical exercise can also shift IgG N-glycome towards a “younger” profile by  
419 increasing IgG galactosylation (26). Although another study reported that prolonged intensive  
420 exercise can have the opposite effect and promote pro-inflammatory changes of IgG N-  
421 glycome (39), its findings are not surprising since it recruited healthy, normal-weight female  
422 participants, subjected to the intense energy deprivation and exercise levels, to induce  
423 substantial fat loss in a rather short time period. The authors also highlighted that starting  
424 weight and the way in which weight loss is achieved could be crucial for the final effect on the  
425 immune system. Therefore, it seems that exercise overall has a positive impact on the immune  
426 system and biological clock, but its intensity and duration should be personalized in order to  
427 provide the optimal results.

428 To summarize, our results indicate that weight loss has impact on inflammation and biological  
429 aging by altering plasma and IgG N-glycosylation patterns. Glycosylation changes can be  
430 reliably quantified and used to estimate the “age” of the immune system. This could represent  
431 a valuable tool in the context of COVID-19 patient stratification. Since inter-individual  
432 variation in protein glycosylation is extensive, its functional implications on membrane  
433 expression of various proteins (including ACE2), functional properties of newly synthesized  
434 SARS-CoV-2 virus particles and regulation of the immune responses may also explain severe  
435 cases of COVID-19 in apparently healthy individuals. A previous research showed that  
436 impairment of ACE2 N-glycosylation affects its ability to allow the transduction of SARS Human  
437 coronavirus NL63 (HCoV-NL63) particles, by disrupting the viral endocytosis (40).

438 Future glycomic studies of patients infected with SARS-CoV-2 would help to elucidate whether  
439 ACE2 N-glycosylation differs in patients with severe COVID-19, compared to asymptomatic  
440 patients or healthy individuals. For the time being, it appears that severity of COVID-19  
441 associates with the majority of obesity-related comorbidity risk factors (41). Therefore, by

442 improving metabolic and endocrine health through weight loss, which consequently  
443 contributes to the preservation of a healthy immune system, one has a best chance to fight  
444 infections.

445

#### 446 **ACKNOWLEDGMENTS**

447 This research was funded by the National Institute for Health Research (NIHR) Oxford  
448 Biomedical Research Centre (BRC). The views expressed are those of the author(s) and not  
449 necessarily those of the NHS, the NIHR or the Department of Health. The authors thank Rachel  
450 Franklin, Michelle Haylock, James Chivenga, Roxanne Williams and the BRC Oxford GI Biobank  
451 for sample collection. The authors thank all the patients who took part in this study.

452

#### 453 **FUNDING**

454 Glycosylation analysis was performed in Genos Glycoscience Research Laboratory and partly  
455 supported by the European Union's Horizon 2020 grants Backup (grant# 777090), European  
456 Structural and Investment Funds IRI grant (#KK.01.2.1.01.0003), Centre of Competence in  
457 Molecular Diagnostics (#KK.01.2.2.03.0006) and Croatian National Centre of Research  
458 Excellence in Personalized Healthcare grant (#KK.01.1.1.01.0010). Bariatric research was  
459 supported by the National Institute for Health Research (NIHR) Oxford Biomedical Research  
460 Centre Gastroenterology and Mucosal Immunity Theme to CVA-C and VLG, Oxford Biomedical  
461 Research Centre Diabetes and Metabolism theme for JWT, MRC programme grant to JWT (ref.  
462 MR/P011462/1), the NIHR Research Capability Funding to VLG and AG, the Wellcome Trust  
463 (101734/Z/13/Z) to AG. NJD is supported by a University of Oxford Novo Nordisk Clinical  
464 Research Fellowship. TwinsUK received funding from the Wellcome Trust European  
465 Community's Seventh Framework Programme (FP7/2007-2013 to TwinsUK); the National  
466 Institute for Health Research (NIHR) Clinical Research Facility at Guy's & St Thomas' NHS  
467 Foundation Trust and the Nottingham NIHR Biomedical Research Centre based at Guy's and  
468 St Thomas' NHS Foundation Trust and King's College London. CM is funded by the MRC AimHy  
469 (MR/M016560/1) project grant and by the Chronic Disease Research Foundation.

470

#### 471 **AUTHOR'S CONTRIBUTION**

472 Study design: CM, AG, CVA-C, GL. Data collection: VLG, ACv, TŠ, NJD, ACi, HD, MF, CM. Data  
473 analysis: DK, FV. Data interpretation: VLG, ACv, TŠ, NJD, DK, FV, MF, JWT, OG, TS, CM, AG,

474 CVA-C, GL. Drafting manuscript: VLG, ACv, TŠ, NJD, DK, FV, GL. Revising and approving final  
475 version of manuscript: ALL. CM, AG, CVA-C and GL take responsibility for the integrity of the  
476 data analysis

477

478

479 **REFERENCES**

- 480 1. Obesity and overweight [Internet]. [cited 2020 Apr 16]. Available from:  
481 <https://www.who.int/news-room/fact-sheets/detail/obesity-and-overweight>
- 482 2. Petrilli CM, Jones SA, Yang J, Rajagopalan H, O'Donnell LF, Chernyak Y, et al. Factors  
483 associated with hospitalization and critical illness among 4,103 patients with COVID-19  
484 disease in New York City. medRxiv. 2020 Apr 11;2020.04.08.20057794.
- 485 3. Garg S. Hospitalization Rates and Characteristics of Patients Hospitalized with  
486 Laboratory-Confirmed Coronavirus Disease 2019 — COVID-NET, 14 States, March 1–30,  
487 2020. MMWR Morb Mortal Wkly Rep [Internet]. 2020 [cited 2020 Apr 26];69. Available  
488 from: <https://www.cdc.gov/mmwr/volumes/69/wr/mm6915e3.htm>
- 489 4. Han TS, Lean ME. A clinical perspective of obesity, metabolic syndrome and  
490 cardiovascular disease. JRSM Cardiovasc Dis. 2016 Dec;5:2048004016633371.
- 491 5. Alpert A, Pickman Y, Leipold M, Rosenberg-Hasson Y, Ji X, Gaujoux R, et al. A clinically  
492 meaningful metric of immune age derived from high-dimensional longitudinal  
493 monitoring. Nat Med. 2019 Mar;25(3):487–95.
- 494 6. Franceschi C, Garagnani P, Parini P, Giuliani C, Santoro A. Inflammaging: a new  
495 immune–metabolic viewpoint for age-related diseases. Nature Reviews Endocrinology.  
496 2018 Oct;14(10):576–90.
- 497 7. Touch S, Clément K, André S. T Cell Populations and Functions Are Altered in Human  
498 Obesity and Type 2 Diabetes. Curr Diab Rep. 2017 Sep;17(9):81.
- 499 8. Dhurandhar NV, Bailey D, Thomas D. Interaction of obesity and infections. Obes Rev.  
500 2015 Dec;16(12):1017–29.
- 501 9. Lauc G, Sinclair D. Biomarkers of biological age as predictors of COVID-19 disease  
502 severity. Aging [Internet]. 2020 Apr 8 [cited 2020 Apr 14]; Available from:  
503 <http://www.aging-us.com/article/103052/text>
- 504 10. Lauc G, Pezer M, Rudan I, Campbell H. Mechanisms of disease: The human N-glycome.  
505 Biochimica et Biophysica Acta - General Subjects. 2016;1860(8):1574–82.
- 506 11. Gornik O, Pavić T, Lauc G. Alternative glycosylation modulates function of IgG and other  
507 proteins - implications on evolution and disease. Biochim Biophys Acta. 2012  
508 Sep;1820(9):1318–26.
- 509 12. Gudelj I, Lauc G, Pezer M. Immunoglobulin G glycosylation in aging and diseases.  
510 Cellular Immunology. 2018;
- 511 13. Dall'Olio F. Glycobiology of aging. In: Subcellular Biochemistry. 2018.
- 512 14. Krištić J, Vučković F, Menni C, Klarić L, Keser T, Beceheli I, et al. Glycans Are a Novel  
513 Biomarker of Chronological and Biological Ages. The Journals of Gerontology: Series A.  
514 2014 Jul;69(7):779–89.



- 515 15. Štambuk J, Nakić N, Vučković F, Pučić-Baković M, Razdorov G, Trbojević-Akmačić I, et al.  
516 Global variability of the human IgG glycome [Internet]. *Biochemistry*; 2019 Feb [cited  
517 2020 Jan 31]. Available from: <http://biorxiv.org/lookup/doi/10.1101/535237>
- 518 16. Menni C, Gudelj I, MacDonald-Dunlop E, Mangino M, Zierer J, Bešić E, et al.  
519 Glycosylation Profile of Immunoglobulin G Is Cross-Sectionally Associated with  
520 Cardiovascular Disease Risk Score and Subclinical Atherosclerosis in Two Independent  
521 Cohorts. *Circulation Research*. 2018;122(11):1555–64.
- 522 17. Wittenbecher C, Štambuk T, Kuxhaus O, Rudman N, Vučković F, Štambuk J, et al. Plasma  
523 N-Glycans as Emerging Biomarkers of Cardiometabolic Risk: A Prospective Investigation  
524 in the EPIC-Potsdam Cohort Study. *Diabetes Care*. 2020 Jan 7;43(3):661–8.
- 525 18. Gao Q, Dolikun M, Stambuk J, Wang H, Zhao F, Yiliham N, et al. Immunoglobulin G N-  
526 Glycans as Potential Postgenomic Biomarkers for Hypertension in the Kazakh  
527 Population. *OmicS*. 2017;21(7):380–9.
- 528 19. Liu J, Dolikun M, Štambuk J, Trbojević-Akmačić I, Zhang J, Wang H, et al. The association  
529 between subclass-specific IgG Fc N-glycosylation profiles and hypertension in the  
530 Uyghur, Kazak, Kirgiz, and Tajik populations. *J Hum Hypertens*. 2018 Sep;32(8–9):555–63.
- 531 20. Wang Y, Klarić L, Yu X, Thaqi K, Dong J, Novokmet M, et al. The Association Between  
532 Glycosylation of Immunoglobulin G and Hypertension: A Multiple Ethnic Cross-Sectional  
533 Study. *Medicine*. 2016 Apr;95(17):e3379.
- 534 21. Nikolac Perkovic M, Pucic Bakovic M, Kristic J, Novokmet M, Huffman JE, Vitart V, et al.  
535 The association between galactosylation of immunoglobulin G and body mass index.  
536 *Progress in Neuro-Psychopharmacology and Biological Psychiatry*. 2014 Jan;48:20–5.
- 537 22. Russell AC, Kepka A, Trbojević-Akmačić I, Ugrina I, Song M, Hui J, et al. Increased central  
538 adiposity is associated with pro-inflammatory immunoglobulin G N-glycans.  
539 *Immunobiology*. 2019;224(1):110–5.
- 540 23. Sundgren NC, Vongpatanasin W, Boggan BMD, Tanigaki K, Yuhanna IS, Chambliss KL, et  
541 al. IgG receptor FcγRIIB plays a key role in obesity-induced hypertension. *Hypertension*.  
542 2015 Feb 21;65(2):456–62.
- 543 24. Tanigaki K, Sacharidou A, Peng J, Chambliss KL, Yuhanna IS, Ghosh D, et al.  
544 Hyposialylated IgG activates endothelial IgG receptor FcγRIIB to promote obesity-  
545 induced insulin resistance. *J Clin Invest*. 2018 Jan 2;128(1):309–22.
- 546 25. Peng J, Vongpatanasin W, Sacharidou A, Kifer D, Yuhanna IS, Banerjee S, et al.  
547 Supplementation with the Sialic Acid Precursor N-acetyl-D-Mannosamine Breaks the  
548 Link Between Obesity and Hypertension. 2019.
- 549 26. Tijardović M, Marijančević D, Bok D, Kifer D, Lauc G, Gornik O, et al. Intense Physical  
550 Exercise Induces an Anti-inflammatory Change in IgG N-Glycosylation Profile. *Frontiers*  
551 *in Physiology*. 2019;10(December):1–10.

- 552 27. Nguyen NT, Kim E, Vu S, Phelan M. Ten-year Outcomes of a Prospective Randomized  
553 Trial of Laparoscopic Gastric Bypass Versus Laparoscopic Gastric Banding. *Ann Surg.*  
554 2018;268(1):106–13.
- 555 28. O’Brien P. Bariatric surgery and type 2 diabetes: a step closer to defining an optimal  
556 approach. *The Lancet Diabetes & Endocrinology.* 2019 Dec 1;7(12):889–91.
- 557 29. Verdi S, Abbasian G, Bowyer RCE, Lachance G, Yarand D, Christofidou P, et al. TwinsUK:  
558 The UK Adult Twin Registry Update. *Twin Res Hum Genet.* 2019 Dec;22(6):523–9.
- 559 30. Pavić T, Dilber D, Kifer D, Selak N, Keser T, Ljubičić Đ, et al. N-glycosylation patterns of  
560 plasma proteins and immunoglobulin G in chronic obstructive pulmonary disease. *J*  
561 *Transl Med.* 2018 Nov 21;16.
- 562 31. Leek JT, Johnson WE, Parker HS, Jaffe AE, Storey JD. The sva package for removing  
563 batch effects and other unwanted variation in high-throughput experiments.  
564 *Bioinformatics.* 2012 Mar 15;28(6):882–3.
- 565 32. R Core Team (2020). R: A language and environment for statistical computing. R  
566 Foundation for Statistical Computing, Vienna, Austria. URL [https://www.R-](https://www.R-project.org/)  
567 [project.org/](https://www.R-project.org/).
- 568 33. Clerc F, Reiding KR, Jansen BC, Kammeijer GSM, Bondt A, Wuhrer M. Human plasma  
569 protein N-glycosylation. *Glycoconj J.* 2016 Jun 1;33(3):309–43.
- 570 34. Bates D, Mächler M, Bolker B, Walker S. Fitting Linear Mixed-Effects Models Using  
571 lme4. *Journal of Statistical Software.* 2015 Oct 7;67(1):1–48.
- 572 35. Clerc F, Novokmet M, Dotz V, Reiding KR, de Haan N, Kammeijer GSM, et al. Plasma N-  
573 Glycan Signatures Are Associated With Features of Inflammatory Bowel Diseases.  
574 *Gastroenterology.* 2018;155(3):829–43.
- 575 36. Novokmet M, Lukić E, Vučković F, –Durić Ž, Keser T, Rajšl K, et al. Changes in IgG and  
576 total plasma protein glycomes in acute systemic inflammation. *Scientific Reports.* 2014  
577 Mar 11;4(1):1–10.
- 578 37. Iida S, Kuni-Kamochi R, Mori K, Misaka H, Inoue M, Okazaki A, et al. Two mechanisms of  
579 the enhanced antibody-dependent cellular cytotoxicity (ADCC) efficacy of non-  
580 fucosylated therapeutic antibodies in human blood. *BMC Cancer.* 2009 Feb 18;9:58.
- 581 38. Kaneko Y, Nimmerjahn F, Ravetch JV. Anti-Inflammatory Activity of Immunoglobulin G  
582 Resulting from Fc Sialylation. *Science.* 2006 Aug 4;313(5787):670–3.
- 583 39. Sarin HV, Gudelj I, Honkanen J, Ihalainen JK, Vuorela A, Lee JH, et al. Molecular  
584 Pathways Mediating Immunosuppression in Response to Prolonged Intensive Physical  
585 Training, Low-Energy Availability, and Intensive Weight Loss. *Front Immunol.*  
586 2019;10:907.
- 587 40. Zhao X, Guo F, Comunale MA, Mehta A, Sehgal M, Jain P, et al. Inhibition of  
588 endoplasmic reticulum-resident glucosidases impairs severe acute respiratory

589 syndrome coronavirus and human coronavirus NL63 spike protein-mediated entry by  
590 altering the glycan processing of angiotensin I-converting enzyme 2. *Antimicrob Agents*  
591 *Chemother.* 2015 Jan;59(1):206–16.

592 41. Maffetone PB, Laursen PB. The Perfect Storm: Coronavirus (Covid-19) Pandemic Meets  
593 Overfat Pandemic. *Front Public Health* [Internet]. 2020 [cited 2020 Apr 24];8. Available  
594 from:  
595 [https://www.frontiersin.org/articles/10.3389/fpubh.2020.00135/full?utm\\_source=F-](https://www.frontiersin.org/articles/10.3389/fpubh.2020.00135/full?utm_source=F-NTF&utm_medium=EMLX&utm_campaign=PRD_FEOPS_20170000_ARTICLE)  
596 [NTF&utm\\_medium=EMLX&utm\\_campaign=PRD\\_FEOPS\\_20170000\\_ARTICLE](https://www.frontiersin.org/articles/10.3389/fpubh.2020.00135/full?utm_source=F-NTF&utm_medium=EMLX&utm_campaign=PRD_FEOPS_20170000_ARTICLE)

597